

# Influence of a diamagnetic impurity on the magnetic properties of the noncollinear antiferromagnet $\text{RbNiCl}_3$

M. E. Zhitomirskii

*L. D. Landau Institute of Theoretical Physics, Russian Academy of Sciences, 142432 Chernogolovka, Moscow Region, Russia; Institute for Solid State Physics, University of Tokyo, Tokyo 106, Japan*

O. A. Petrenko

*Department of Physics and Astronomy, McMaster University, Hamilton Ontario L8S 4M1, Canada*

S. V. Petrov, L. A. Prozorova, and S. S. Sosin

*P. L. Kapitza Institute of Physical Problems, Russian Academy of Sciences, 117334 Moscow, Russia*  
(Submitted 17 February 1995)

*Zh. Éksp. Teor. Fiz.* **108**, 343–355 (July 1995)

The static and resonant properties of the diluted antiferromagnet  $\text{RbNiCl}_3:1\% \text{Mg}$  have been investigated. The impurity has been observed to significantly influence the antiferromagnetic resonance spectrum, as well as the magnetization in the region of the spin-flip transition. All the effects observed have been described using a phenomenological approach based on the exchange symmetry of the magnetic system, taking into account relativistic invariants of higher order in  $v^2/c^2$ . Qualitative agreement with experiment has been achieved in a microscopic model by introducing a two-ion anisotropy of the form  $\hat{D}(S_i^z)^2(S_j^z)^2$  into the spin Hamiltonian. It has been postulated that an impurity which does not occupy a site in the crystal lattice strongly distorts the electrical interactions within the crystal, altering the character of the anisotropic interactions. © 1995 American Institute of Physics.

## 1. INTRODUCTION

An efficient way to obtain magnetic systems with new static and resonant properties is to introduce different quantities of a nonmagnetic impurity into a pure structure. The presence of an impurity results either in mechanical distortion of the structure of the original crystal or in disruption of some part of the interaction between the magnetic atoms, which is reflected in the collective behavior of the spin system. There have been numerous studies of the properties of diluted antiferromagnets. Many of them were devoted to phenomena associated with weakening of the molecular field due to a decrease in the number of interacting atoms and therefore noticeable only when the concentration of the impurity is sufficiently large.<sup>1</sup> However, when noncollinear antiferromagnets such as  $\text{CsNiCl}_3$  are diluted, the appearance of less trivial effects, which have a considerably stronger influence on their properties, is possible. This is due primarily to the character of the exchange ordering, which is organized in such a manner that the spins lying in the basal plane of the crystal are directed at  $\approx 120^\circ$  angles to one another, i.e., the minimum of the exchange energy is achieved for the entire system as a whole, rather than for each pair of spins individually. Such systems are frustrated, and when the crystal lattice is distorted, great changes result, up to and including incommensurability.

In addition, even a small number of impurity atoms can distort the crystal field and alter the electronic configuration of the magnetic ions, which should influence the anisotropic interactions in the original structure. It should be taken into account here that the easy-axis anisotropy of antiferromagnets like  $\text{CsNiCl}_3$ , which is generally described in the effec-

tive single-ion form  $D\Sigma(S_i^z)^2$ , most likely consists of several contributions.<sup>2</sup> The single-ion anisotropy appearing as a result of splitting of the ground-state term of the magnetic ion  $\text{Ni}^{2+}$  ( ${}^3F$ ) in an axial crystal field is of the easy-plane type. Therefore, there should be at least one more anisotropic interaction, for example, two-ion anisotropy of the form  $-D_1\Sigma S_i^z S_j^z$ , which is usually called “exchange anisotropy.” The anisotropy actually observed is the result of the competition between two opposing contributions and is, therefore, sensitive to even small changes in one of them.

Other macroscopic manifestations of dilution can also be associated with features of the magnetic and crystal structure of these compounds, for example, their quasi-one-dimensional character.

In this work we investigated the static and resonant properties of the antiferromagnet  $\text{RbNiCl}_3$ , already thoroughly studied diluted with a small quantity of a diamagnetic impurity. After phenomenologically describing the observed changes in the magnetic properties<sup>3</sup> and comparing the results obtained with the predictions of spin-wave theory on the basis of the standard spin Hamiltonian

$$\mathcal{H} = \sum J_{ij} S_i S_j + \sum J'_{ij} S_i J_j - D \sum (S_i^z)^2 - \gamma H \sum S_i \quad (1)$$

we can understand how Eq. (1) can be modified to achieve optimal agreement between the two approaches. This allows us to advance a hypothesis regarding the microscopic nature of the observed effects.



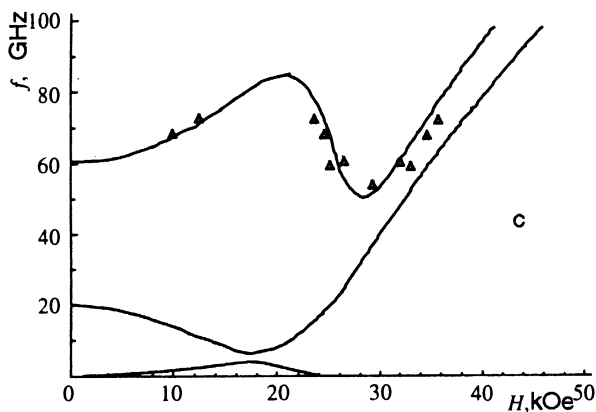
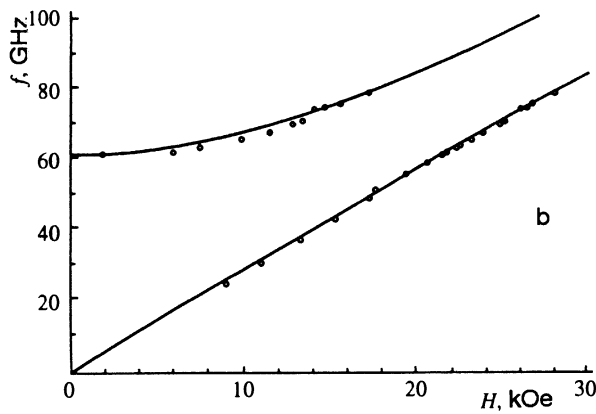
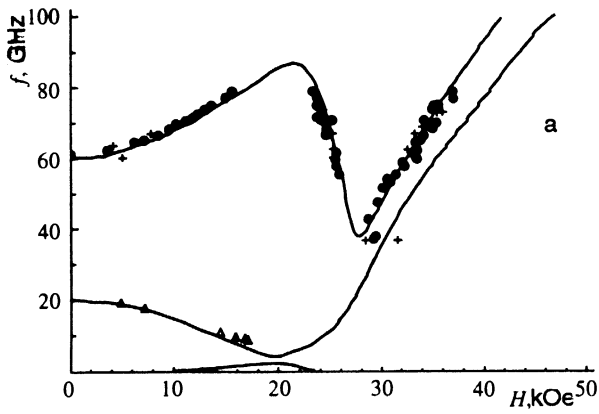


FIG. 2. Resonance spectrum of RbNiCl<sub>3</sub>:1% Mg for  $H \parallel C_6$  (a),  $H \perp C_6$  (b), and  $\angle(C_6, H) \approx 5^\circ$  (c). Solid curves—data from theoretical calculations.

exchange structure, the calculated gap for the pure crystal being  $\omega_3(0) = 240$  MHz. Experimental plots of the resonant field versus  $\varphi$  are presented for two frequencies in Figs. 3a and 3b.

For  $H \perp C_6$  (Fig. 2b) no fundamental changes were discovered in the spectrum [apart from, of course, the corresponding increase in the gap  $\omega_1(0)$ ]. Although the spectrum for an intermediate orientation of the field relative to the  $C_6$  axis (Fig. 2c) likewise does not show any fundamental differences from the original spectrum, it cannot be de-

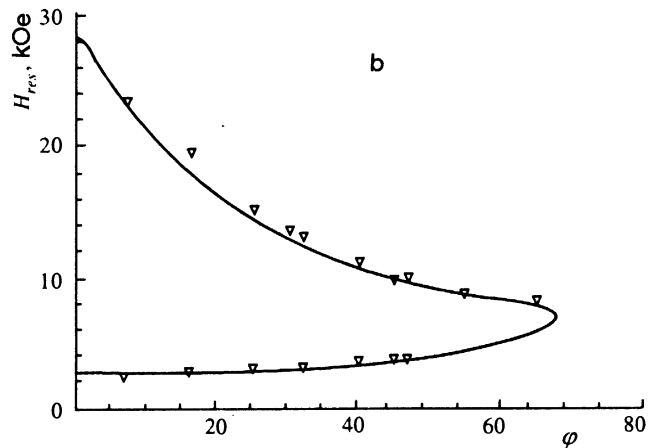
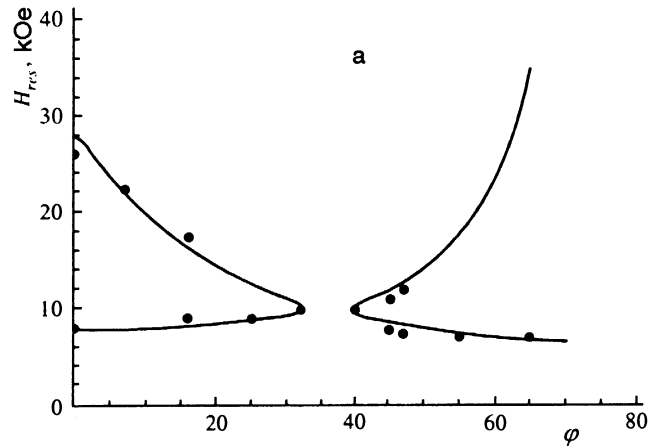


FIG. 3. Angular dependence of the resonant field for the  $\omega_2$  and  $\omega_3$  branches at 17 GHz (a) and 19.5 GHz (b). Solid curves—theoretical calculation with the fitted constants  $a_1$  and  $a_2$ .

scribed in the approach of Ref. 5 by varying the phenomenological constants  $\eta$  and  $H_c$  and the tilt angle  $\varphi$ .

The Néel temperature remained unchanged from pure RbNiCl<sub>3</sub>, in which  $T_N \approx 11$  K.

## 2.2. Measurement of the static magnetization

Besides investigating the resonant properties of RbNiCl<sub>3</sub>:1% Mg, we performed a series of static measurements on a vibrating magnetometer for the purpose of revealing the behavior of the magnetization at the critical fields. The field dependence of the components of the magnetization parallel and perpendicular to the external magnetic field was investigated at two temperatures (1.8 K and 4.2 K). The external field was applied along the  $x$  axis. The measuring coils recorded the magnetization along the  $x$  and  $y$  axes. The  $C_6$  axis was aligned at a certain angle  $\varphi$  to the  $x$  axis. The angle  $\xi$  between the  $C_6$  and  $z$  axis is one of the systematic experimental errors which can be taken into account. The angle  $\theta$  between the projection of  $C_6$  onto the  $xy$  plane and the  $x$  axis was varied during the measurements. The anisotropy of the crystal causes magnetization to appear not only along the field ( $M_x$ ), but also in the perpendicular direction

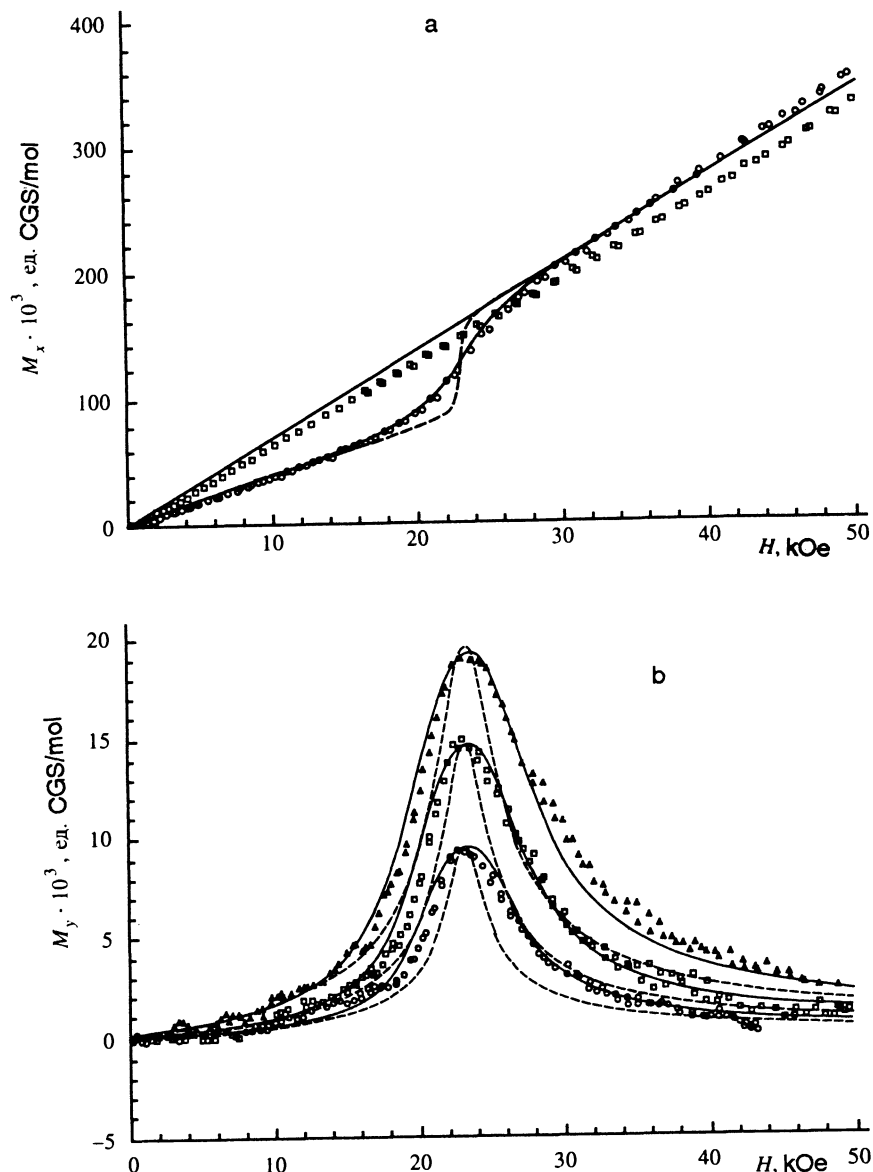


FIG. 4. (a) Dependence of the parallel component of the magnetization ( $M_x$ ) for  $H \parallel C_6$  and  $H \perp C_6$ . Dashed line—calculation using the approximation in Ref. 3; solid lines—calculation in the final model. (b) Dependence of the perpendicular component of the magnetization ( $M_y$ ) for several values of  $\theta$  ( $\circ$ — $1^\circ$ ,  $\square$ — $2^\circ$ ,  $\triangle$ — $3^\circ$ ). Dashed lines—calculation using the approximation in Ref. 3, solid lines—calculation in the final model.

( $M_y$ ) when an external magnetic field is applied. The corresponding equations are presented in the next section.

Figure 4a shows plots of  $M_x(H)$  at  $T=1.8$  K for  $C_6 \parallel H$  [ $\angle(C_6, H) \approx \xi$ ] and  $C_6 \perp H$ , and Fig. 4b presents plots of  $M_y(H)$  for various values of  $\theta$  ( $1^\circ$ ,  $2^\circ$ ,  $3^\circ$ ). The plot of  $M_x(H)$  for  $H \parallel C_6$  does not exhibit an abrupt jump in the magnetization corresponding to a spin-flip phase transition of the first kind, instead of which there is smooth variation of  $M_x$  over an interval of  $\sim 5$  kOe with respect to the field. The plots of  $M_y(H)$  for all the values of the angle are also broadened considerably in comparison with the analogous data for the pure crystal.

### 3. PHENOMENOLOGICAL DESCRIPTION OF $\text{CsNiCl}_3$ ANTIFERROMAGNETS

The phenomenological approach to the description of the magnetic properties of crystals can be based only on the symmetry of the crystal structure;<sup>7</sup> however, it is far more convenient to use the symmetry of the magnetic ordering in

the exchange approximation. The latter method is applicable, if the relativistic interactions in the system (spin-orbit, dipole-dipole, etc.) can be treated as small perturbations in comparison with the exchange forces. Such an assumption is generally justifiable, making it possible to describe the static and resonant properties with comparative ease without resorting to concrete model representations.<sup>8</sup> This was done on a theoretical level for the first time in Ref. 3 and was subsequently applied to the calculation of the acoustic magnetic resonance modes in  $\text{CsNiCl}_3$ , good agreement with experiment being achieved by introducing a relativistic invariant to first order in  $v^2/c^2$  (Ref. 5).

However, in the general case this is not enough. For example, when systems with strong distortions of the  $120^\circ$ -exchange structure due to anisotropy are considered, third-order invariants which remove the degeneracy in the spin plane must be taken into account. The phenomenological description of such a system was demonstrated in Ref. 9, where the spectrum of the easy-axis antiferromagnet

CsMnI<sub>3</sub> with strong anisotropy was measured and calculated. It is also impossible to describe the experimental results obtained in the present work without introducing high-order relativistic invariants.

The exchange spin structure of systems of the CsNiCl<sub>3</sub> type is described by the helicoid

$$\mathbf{S} \sim \mathbf{l}_1 \cos \mathbf{k} \cdot \mathbf{r} + \mathbf{l}_2 \sin \mathbf{k} \cdot \mathbf{r}, \quad (2)$$

where  $\mathbf{l}_1$  and  $\mathbf{l}_2$  are unit vectors (of the polarization) and  $\mathbf{k}$  is the spatial wave vector determined by minimization of the exchange energy [in the present case  $\mathbf{k} = (2\pi/3a, 2\pi/3a, \pi/c)$ ]. In the absence of a magnetic field all the spins lie in the plane perpendicular to the vector  $\mathbf{n} = \mathbf{l}_1 \times \mathbf{l}_2$ .

The dynamics of the system is defined by the Lagrangian

$$\mathcal{L} = \frac{\chi_{\perp}}{2\gamma^2} (\mathbf{\Omega} + \gamma \mathbf{H})^2 + \frac{\eta \chi_{\perp}}{2\gamma^2} [\mathbf{n} \cdot (\mathbf{\Omega} + \gamma \mathbf{H})]^2 - U_a, \quad (3)$$

where we have written  $\eta = (\chi_{\parallel} - \chi_{\perp})/\chi_{\perp}$ ,  $\mathbf{\Omega}$  is the angular rotation rate in spin space, and  $U_a$  is the anisotropy energy, in which we take into account invariants to first, second, and third order in  $v^2/c^2$ :

$$U_a = \frac{\alpha}{2} n_z^2 + \frac{\beta}{4} n_z^4 + U^{(3)}. \quad (4)$$

For an easy-axis structure  $\alpha > 0$ ,  $\beta$  has an arbitrary sign ( $\beta > -2\alpha$ ), and the specific form of  $U^{(3)}$  is discussed below.

We first consider the static behavior of a system described by the Lagrangian (3) with anisotropy energy (4), in which, for simplicity, we take into account only the first two terms. In this case we have  $\mathbf{\Omega} \equiv 0$ ,  $\angle(C_6, \mathbf{H}) = \varphi$ ,  $\angle(C_6, \mathbf{n}) = \psi$ , and (3) takes the form

$$\begin{aligned} \mathcal{L} = & \frac{\chi_{\perp}}{2} H^2 \cos^2 \varphi + \frac{\eta \chi_{\perp} H^2}{2} \cos^2(\psi - \varphi) - \frac{\alpha}{2} \cos^2 \psi \\ & - \frac{\beta}{4} \cos^4 \psi. \end{aligned} \quad (5)$$

Under the condition  $\beta > 0$ , the minimization of (5) with respect to  $\psi$  at  $\varphi = 0$  gives:

$$\psi = \frac{\pi}{2} \text{ for } H^2 < \frac{\alpha}{\eta \chi_{\perp}} = H_{c_1}^2, \quad (6.1)$$

$$\psi = \arccos \sqrt{\frac{\eta \chi_{\perp} H^2 - \alpha}{\beta}} \text{ for } H_{c_1}^2 < H^2 < \frac{\alpha + \beta}{\eta \chi_{\perp}} = H_{c_2}^2, \quad (6.2)$$

$$\psi = 0 \text{ for } H^2 > H_{c_2}^2. \quad (6.3)$$

As we see, consideration of the invariant  $\beta n_z^4/4$  causes the spin-flip transition to disappear and an intermediate range

of fields to appear, in which the spin plane turns smoothly from the  $\mathbf{n} \perp C_6$  orientation to the  $\mathbf{n} \parallel C_6$  orientation. Such turning is accompanied by two symmetry violations, which suggest the occurrence of phase transitions of the second kind at  $H = H_{c_1}$  and  $H = H_{c_2}$ .

Next, the value of  $\psi$  found is substituted into the original Lagrangian, and then the components of the magnetization in the coordinate system associated with the crystal  $\mathbf{M} = -(\partial \mathcal{L} / \partial \mathbf{H})$  is easily found. The empirical values of  $M_x$  and  $M_y$  (see the preceding section) are related to  $\mathbf{M}$  by ordinary rotation formulas. Such an analytical calculation in the approximation in Ref. 3 gives the following expressions for  $M_x$  and  $M_y$ :

$$\begin{aligned} M_z = & \left( \chi_{\perp} + \frac{\eta \chi_{\perp}}{2} \right) H \\ & + \frac{\eta \chi_{\perp} H}{2} \left( \frac{H^2 - H_c^2 \cos 2\varphi}{\sqrt{H^4 - 2H^2 H_c^2 \cos 2\varphi + H_c^4}} \right) \\ M_y = & \frac{\eta \chi_{\perp} H H_c^2 \cos^2 \xi \sin 2\theta}{2\sqrt{H^4 - 2H^2 H_c^2 \cos 2\varphi + H_c^4}}. \end{aligned} \quad (7)$$

The analogous calculation with consideration of the invariant  $\beta n_z^4/4$  is technically difficult and was therefore performed numerically. The results for a fixed value of  $\xi$  and several values of  $\theta$  were presented in the preceding section in Figs. 4a and 4b.

We proceed to a calculation of the spectrum of a diluted antiferromagnet, at first without consideration of the third-order invariants. To obtain linearized equations of motion, the variables  $\mathbf{n}$  and  $\mathbf{\Omega}$  appearing in (3) must be expanded to second-order terms in the small rotation angle  $\theta$

$$\mathbf{n} = \mathbf{n}_0 + [\boldsymbol{\theta} \times \mathbf{n}_0] + \frac{1}{2} \boldsymbol{\theta} \times \boldsymbol{\theta} \times \mathbf{n}_0,$$

$$\mathbf{\Omega} = \dot{\boldsymbol{\theta}} + \frac{1}{2} \boldsymbol{\theta} \times \dot{\boldsymbol{\theta}}, \quad (8)$$

where  $\mathbf{n}_0$  is determined from equilibrium conditions (6).

Varying the Lagrangian, we obtain a system of equations, from which the fundamental frequencies of the fluctuations are found. For  $H < H_{c_1}$  and  $H > H_{c_2}$  the results coincide exactly with Ref. 5, if  $H_c$  is replaced by  $H_{c_1}$  and  $H_{c_2}$ , respectively. The intermediate range of fields  $H_{c_1} < H < H_{c_2}$ , in which the spin plane turns according to (6.2), is of interest in itself. The resonant frequencies are specified by the characteristic equation

$$\begin{vmatrix} \omega^2 & -i\omega H(1-\eta)\cos\psi & 0 \\ i\omega H(1-\eta)\cos\psi & \omega^2 - 2\eta(H^2 - H_c^2)\sin^2\psi & i\omega H(1+\eta)\sin\psi \\ 0 & -i\omega H(1+\eta)\sin\psi & \omega^2(1+\eta) \end{vmatrix} = 0,$$

whence the only nonzero frequency  $\omega_1$  in the present approximation is easily found:

$$\left(\frac{\omega_1}{\gamma}\right)^2 = \frac{H^2(H_{c_2}^2 - H_{c_1}^2) + \eta(2H_{c_1}^2 H_{c_2}^2 - H^4 - H^2 H_{c_2}^2) + \eta^2(H^2 - H_{c_1}^2)}{H_{c_2}^2 - H_{c_1}^2}. \quad (9)$$

The lower relativistic branch corresponds to fluctuations in the spin plane; therefore, to describe it, the invariants which orient spins in the plane and cause the appearance of the corresponding gap in the spectrum must be taken into account in the anisotropy energy. As was shown in Ref. 9, the predominant orientation of the spins is determined by four different third-order invariants. We use  $g_i/12$  to denote the constants in front of them. Then, when  $H \parallel C_6$  holds the following expression for  $\omega_3(H)$  is obtained from the Euler-Lagrange equations:

$$\omega_3^2(H) = \frac{\gamma^2}{\chi_\perp} \frac{6\eta}{1 + \eta} \frac{H_c^2 - H^2}{\eta H_c^2 + H^2} (g_1 + g_2 H^2 + g_3 H^4 + g_4 H^6), \quad (10)$$

satisfactory agreement with experiment being achieved already when  $g_1$  and  $g_2$  are taken into account. To obtain the general equations of motion for the intermediate range of fields  $H_{c1} < H < H_{c2}$  and an arbitrary value of  $\varphi$ , we must take into account the third-order invariants in finding the equilibrium value of  $\psi$  and consider their contribution to the zeroth matrix elements of the original equation. However, to avoid exceeding the accuracy,  $\psi$  should be substituted in its original form into the final expressions for  $\omega_{2,3}^2$ . The equilibrium value of  $\psi$  for an arbitrary direction of the field relative to the  $C_6$  axis is determined from the equation

$$H_1^2 \sin 2\psi + H_0^2 \sin 2\psi \cos^2 \psi - H^2 \sin 2(\psi - \varphi) = 0, \quad (11)$$

with  $H_0^2 = H_2^2 - H_1^2$ , which can be solved only numerically, and then the values of  $\psi$  found are plugged into the expression for the resonant frequencies the characteristic equation can therefore be written in the form

$$\det \|A_{ij}\| = 0, \quad (12)$$

$$A_{11} = \omega^2 - \eta H^2 \cos^2(\psi - \varphi) + \eta H_1^2 \cos^2 \psi + \eta H_0^2 \cos^4 \psi - 5a_1 \sin^4 \psi \cos^2 \psi - \frac{a_2 H^2}{3} \left( 2 \sin^2 \psi \sin 2\psi \sin 2(\psi - \varphi) + \frac{3}{2} \sin^2 2\psi \sin^2(\psi - \varphi) + \sin^4 \psi \cos^2(\psi - \varphi) \right),$$

$$A_{22} = \omega^2 - \eta H^2 \cos 2(\psi - \varphi) + \eta H_1^2 \cos 2\psi + \eta H_0^2 \cos^2 \psi (1 - 4 \sin^2 \psi),$$

$$A_{33} = \omega^2 (1 + \eta) - 6a_1 \sin^6 \psi - 6a_2 H^2 \sin^4 \psi \sin^2(\psi - \varphi),$$

$$A_{12} = -A_{21} = i\omega H (1 - \eta) \cos(\psi - \varphi),$$

$$A_{13} = A_{31} = -6a_1 \sin^5 \psi \cos \psi - 2a_2 H^2 \sin^3 \psi \left( 2 \sin^2(\psi - \varphi) \cos \psi + \frac{1}{2} \sin \psi \sin 2(\psi - \varphi) \right),$$

$$A_{32} = -A_{23} = i\omega H (1 + \eta) \sin(\psi - \varphi),$$

where the notation  $a_i = g_i/\chi_\perp$  has been introduced.

All the results of the numerical calculation of the spectrum and its angular dependences with the fitted phenomenological parameters  $\eta$ ,  $H_{c1,2}$ , and  $a_i$  are presented in Figs. 2 and 3.

#### 4. DISCUSSION

All the phenomenological constants introduced can be determined by applying the approach described in the preceding section to the available experimental data. Figures 4a and 4b present the data from the static measurements, which most graphically demonstrate the impossibility of describing the spin-flip region of doped RbNiCl<sub>3</sub> without introducing two phase transitions of the second kind instead of the spin-flip transition. In addition,  $M_y(H)$  provides the most reliable estimates for  $H_{c1}$  and  $H_{c2}$ , since  $M_y$  differs from zero only when  $\mathbf{n}$  has an intermediate position ( $0 < n_z < 1$ ) and, in this sense, is a pure indicator of the effect. The data from the numerical calculation are presented with the parameters  $H_{c1} = 20.8$  kOe and  $H_{c2} = 26.0$  kOe. The difference between the heights of the peaks is caused by the nonzero value of  $\xi$  and gives  $\xi \approx 3.0^\circ$ .

The same parameters should be used to describe the resonance spectrum. For good agreement between the branch  $\omega_1(H)$  with experiment at  $T = 1.6$  K at all orientations of the field relative to the  $C_6$  axis, it is sufficient to set  $\eta = 0.86$ . The gap of the lower branch  $\omega_3(0)$  is determined by the invariant  $a_1$ , whence we find  $a_1 = 120$  GHz<sup>2</sup>, but its behavior in a field also depends on the third-order field invariants. It turns out that for a satisfactory description of all the available experimental data (including the angular dependence of the resonant field at a given frequency) it is sufficient to introduce the constant  $a_2 = -0.022$  and to set  $a_3$  and  $a_4$  equal to zero. All the theoretical dependence with the phenomenological parameters indicated is shown in the respective figures. It is noteworthy that the accuracy of the determination of  $a_2$  is fairly low, since it determines only the character of the field and angular dependences of the lower branch.

The results obtained attest to the significant influence of the impurity on the electrical interactions within the crystal, which causes dramatic changes in the magnetic anisotropy. However, such a conclusion cannot serve as a basis for understanding the causes of this influence. Moreover, the behavior of the system, which is determined by a large number of fundamentally independent parameters, is fairly arbitrary in the general case. To eliminate these problems, the existing phenomenological approach can be associated with a particular microscopic model. At  $T = 0$ , the original (undiluted) magnetic structure is described well by the Hamiltonian (1). However, impurities have such a strong influence on it that

even a qualitative explanation for the observed results becomes impossible with such a model. There are several general models for modifying the Hamiltonian of stochastically diluted systems. First of all, the exchange sums can be "diluted" by randomly excluding a certain number of interactions from them. In the mean-field approximation this naturally results in decreases in the exchange constants by an amount on the order of the concentration, i.e., produces a tiny effect opposing the observed effect. Since  $T_N$  did not vary from the case of pure  $\text{RbNiCl}_3$ , we assumed that the influence of the impurity on the exchange interactions is negligibly small. When other model restrictions were considered, it was found that qualitative agreement with experiment can be achieved by introducing anisotropy of the form

$$U_a = D \sum (S_i^z)^2 - 2D_1 \sum (S_i^z)^2 (S_j^z)^2 \quad (13)$$

into the Hamiltonian.

The appearance of a fourth-degree term in  $S_z$  can be conditioned either by the influence of an impurity not occupying sites in the lattice on the crystal field of the sample or by distortion of the electronic configuration of the magnetic atoms with resultant alteration of the two-ion anisotropy. Naturally, quadratic two-ion anisotropy of the form  $D'_{ij} S_i^z S_j^z$  must also be introduced into the Hamiltonian, but its contribution cannot be distinguished from the single-ion anisotropy; therefore it does not produce anything besides a change in the effective constant  $D$ .

Now it is not difficult to relate the phenomenological and microscopic constants by comparing the potential energy of the Lagrangian and the Hamiltonian. It should be recalled here that the total potential energy of the spin system is taken into account in (13), while the potential energy in (3) and (4) is calculated relative to the ground-state energy. Therefore, in each individual case we must select a parameter which can be used to express the change in the potential energy of the Hamiltonian when the system undergoes virtual deviation from the equilibrium position and compare it to the corresponding terms in (4) (see Ref. 9). For the constants in front of the invariants describing the fluctuations of the spin plane (the vector  $\mathbf{n}$ ), we obtain

$$\alpha = DS^2 - \frac{3}{2} D_1 S^4, \quad \beta = \frac{3}{2} D_1 S^4, \quad (14)$$

whence we have

$$1 - \frac{H_{c1}^2}{H_{c2}^2} = \frac{3}{2} \frac{D_1 S^2}{D}, \quad (15)$$

and for the constants in front of the invariants corresponding to the fluctuations of the spins in the plane, we have

$$g_1 = \frac{D_1 S^4}{6J'} (D - D_1 S^2), \quad g_2 = -\frac{D_1 S^2}{96J'J}, \quad g_{3,4} \approx 0. \quad (16)$$

Now the expression for  $\omega_3$  takes the specific form

$$\omega_3^2(H) \approx \frac{\gamma^2 \eta A (H_{c1}^2 - H^2)(H_3^2 - H^2)}{1 + \eta \frac{\eta H_{c1}^2 + H^2}{\eta H_{c1}^2 + H^2}}, \quad (17)$$

where  $A = D_1 S^2 / J'$  and  $H_3^2 = 16JS^2(D - D_1 S^2)$ , i.e., it lies between  $H_{c1}$  and  $H_{c2}$ .

The expression for the gap  $\omega_3(0)$  can be written in the form

$$\omega_3(0) = \frac{\omega_1^2(0)}{12S\sqrt{JJ'}} \sqrt{(k-1)(k+2)}, \quad (18)$$

where  $k = (H_{c2}/H_{c1})^2$ .

The constants  $D$  and  $D_1$  can be chosen independently with respect to any parameters. We calculate  $D$  and  $D_1$  from the critical fields  $H_{c1}$  and  $H_{c2}$  and the new value of the upper relativistic gap. From Eq. (15) we find the relation  $D_1 S^4 \approx 0.24DS^2$ , and from  $H_{c2}$  we obtain  $DS^2 = 0.94$  GHz, whence we find  $D_1 S^4 \approx 0.22$  GHz. Using the values of  $J$  and  $J'$  obtained in Ref. 6 or Ref. 10, we find the value of the lower gap  $\omega_3(0) = 4.2$  GHz or 6 GHz, respectively, i.e., a value three to five times smaller than the experimental value. Nevertheless, this simple modification of the anisotropy in the Hamiltonian (1) makes it possible, first, to account for the replacement of the spin-flip transition by two phase transitions of the second kind and, second, to increase the value of the gap of the lower relativistic branch by an order of magnitude, i.e., to achieve qualitative agreement with the observed results.

The fairly considerable disparity between the calculation and experiment for the lower branch can be attributed to several factors. It is simplest to postulate that the anisotropy of the form (13) introduced into the Hamiltonian is too simple to describe the changes in the electrical interactions that occur due to impurities. In this case it is reasonable to reject the microscopic model and restrict ourselves to the more general phenomenological description.

However, two other possibilities should be considered. First, Eqs. (17)–(18) were obtained in the classical approximation. This means that the field dependences of the relativistic branches, which are determined only by the symmetry of the magnetic structure, were found correctly, and that the constants  $J$ ,  $J'$ ,  $D$ , and  $D_1$  appearing in the gap are assumed to be renormalized. Of course, the values of the gaps can still be reconciled formally by varying the exchange constants (in the present case this gives the unjustifiably small value  $J' \approx 2$  GHz). However, the classical equations were found without consideration of the possible differences in the renormalization for different branches. For this reason, it would be interesting to measure  $\omega_3$  in pure  $\text{RbNiCl}_3$  and to ascertain whether the relations between the relativistic branches found from the Hamiltonian (1) hold with the constants taken from Refs. 6, 8, or 10. It should be noted that similar measurements have been performed in other easy-axis structures [ $\text{CsNiCl}_3$  (Refs. 8 and 11) and  $\text{CsMnI}_3$  (Ref. 9)]. Two fundamentally different values were obtained for  $\text{CsNiCl}_3$ :  $\omega_3(0) \approx 20$  GHz and  $\omega_3(0) \approx 1$  GHz, respectively. The reasonable value  $J' \approx 8$  GHz is obtained only from Ref. 11, no definite conclusions can be drawn regarding the applicability of the classical approximation due to the inadequate accuracy of these results. The experimental data for  $\text{CsMnI}_3$  also exhibit a significant departure from the classical calculation, which can be eliminated only by modifying the Hamiltonian (1).

Second, since the lower branch is caused by the nonideal nature of the  $120^\circ$  structure, its nonzero value in the pure crystal is determined by the smallness of the relativistic interactions in comparison with the interchain exchange. The presence of impurities possibly causes some regular distortions of the spin exchange structure (for example, due to its frustration), as a result of which the influence of the anisotropy is enhanced, and  $\omega_3(0)$  can increase dramatically.

In conclusion, we thank M. I. Kaganov, V. I. Marchenko, and I. A. Zaliznyak for their useful advice and for discussing the problem, as well as Yu. M. Tsipenyuk and A. N. Bazhan for their assistance in performing the experiments.

This research was partially supported by the Soros International Science Foundation (grant No. M3K000) and the Russian Fund for Fundamental Research (project No. 93-02-03225). M. E. Zh. thanks the JSPS for partial financial support.

<sup>1</sup>E. C. Svensson, T. M. Holden, W. J. L. Buyers *et al.*, *Solid State Commun.* **7**, 1693 (1969).

- <sup>2</sup>A. Harrison and D. Visser, *J. Phys.: Condens. Matter* **4**, 6977 (1992).  
<sup>3</sup>A. F. Andreev and V. I. Marchenko, *Usp. Fiz. Nauk* **130**, 39 (1980) [*Sov. Phys. Usp.* **23**, 21 (1980)].  
<sup>4</sup>A. N. Bazhan, A. S. Borovik-Romanov, and N. M. Kreines, *Prib. Tekh. Éksp.* **1**, 412 (1973).  
<sup>5</sup>I. A. Zaliznyak, V. I. Marchenko, S. V. Petrov, L. A. Prozorova, and A. V. Chubukov, *Pis'ma Zh. Éksp. Teor. Fiz.* **47**, 172 (1988) [*JETP Lett.* **47**, 211 (1988)].  
<sup>6</sup>O. A. Petrenko, S. V. Petrov, and L. A. Prozorova, *Zh. Éksp. Teor. Fiz.* **98**, 727 (1990) [*Sov. Phys. JETP* **71**, 406 (1990)].  
<sup>7</sup>I. E. Dzyaloshniski, *Zh. Éksp. Teor. Fiz.* **47**, 992 (1964) [*Sov. Phys. JETP* **20**, 665 (1965)].  
<sup>8</sup>H. Tanaka, S. Teraoka, E. Kakehashi *et al.*, *J. Phys. Soc. Jpn.* **57**, 3979 (1988).  
<sup>9</sup>S. I. Abarzhi, M. E. Zhitomirskii, O. A. Petrenko *et al.*, *Zh. Éksp. Teor. Fiz.* **104**, 3232 (1993) [*JETP* **77**, 521 (1993)].  
<sup>10</sup>Z. Tun, W. J. L. Buyers, A. Harrison, and J. A. Rayne, *Phys. Rev. B* **43**, 13 331 (1991).  
<sup>11</sup>I. A. Zaliznyak, L. A. Prozorova, and A. V. Chubukov, *J. Phys.: Condens. Matter* **1**, 4743 (1989).

Translated by P. Shelnitz